Article

Traversable wormhole dynamics on a quantum processor

https://doi.org/10.1038/s41586-022-05424-3

Received: 22 February 2022

Accepted: 7 October 2022

Published online: 30 November 2022

Check for updates

Daniel Jafferis[1,7], Alexander Zlokapa[2,3,4,5,7], Joseph D. Lykken[6], David K. Kolchmeyer[1], Samantha I. Davis[3,4], Nikolai Lauk[3,4], Hartmut Neven[5] & Maria Spiropulu[3,4]✉

The holographic principle, theorized to be a property of quantum gravity, postulates that the description of a volume of space can be encoded on a lower-dimensional boundary. The anti-de Sitter (AdS)/conformal field theory correspondence or duality[1] is the principal example of holography. The Sachdev–Ye–Kitaev (SYK) model of $N \gg 1$ Majorana fermions[2,3] has features suggesting the existence of a gravitational dual in AdS_2, and is a new realization of holography[4–6]. We invoke the holographic correspondence of the SYK many-body system and gravity to probe the conjectured ER=EPR relation between entanglement and spacetime geometry[7,8] through the traversable wormhole mechanism as implemented in the SYK model[9,10]. A qubit can be used to probe the SYK traversable wormhole dynamics through the corresponding teleportation protocol[9]. This can be realized as a quantum circuit, equivalent to the gravitational picture in the semiclassical limit of an infinite number of qubits[9]. Here we use learning techniques to construct a sparsified SYK model that we experimentally realize with 164 two-qubit gates on a nine-qubit circuit and observe the corresponding traversable wormhole dynamics. Despite its approximate nature, the sparsified SYK model preserves key properties of the traversable wormhole physics: perfect size winding[11–13], coupling on either side of the wormhole that is consistent with a negative energy shockwave[14], a Shapiro time delay[15], causal time-order of signals emerging from the wormhole, and scrambling and thermalization dynamics[16,17]. Our experiment was run on the Google Sycamore processor. By interrogating a two-dimensional gravity dual system, our work represents a step towards a program for studying quantum gravity in the laboratory. Future developments will require improved hardware scalability and performance as well as theoretical developments including higher-dimensional quantum gravity duals[18] and other SYK-like models[19].

Traversable wormholes[10,14] provide a causal probe of the ER=EPR relation[7] between entanglement and geometry through the holographic duality[1,20,21]. In this construction, a pair of black holes in a thermofield double (TFD) state have their interiors connected by an Einstein–Rosen bridge. Classically, the null energy condition prevents such wormholes from being traversable[22–25]. The basic mechanism found in ref. [14] is that the gravitational backreaction to quantum effects induced by couplings between the exterior regions of the pair of black holes can render the wormhole traversable[26]. It was demonstrated by refs. [10,14] that sending quantum information through such a wormhole is the gravitational description of quantum teleportation in the dual many-body system: the physical picture behind this teleportation is that the qubit traverses the emergent wormhole. As described by the size-winding mechanism[11,12], information placed in the wormhole is scrambled throughout the left subsystem, then the weak coupling between the two sides of the wormhole causes the information to unscramble and refocus in the right subsystem. Owing to the chaotic nature of such scrambling–unscrambling dynamics, the many-body time evolution must be implemented with high fidelity to transmit information through the wormhole. In this work, we demonstrate the experimental realization of traversable wormhole dynamics on nine qubits with 164 two-qubit gates on the Google Sycamore processor [27].

Considering gravity with nearly AdS_2 boundary conditions[28] as the dual to a quantum system, the TFD state corresponds to an anti-de Sitter (AdS)-Schwarzschild wormhole[29]. Two quantum systems—denoted L and R for the two black holes—are entangled in the TFD state at temperature $1/\beta$. In the gravitational picture, a qubit is injected into L at time $-t_0$ and arrives at R at t_1 due to a coupling interaction at $t = 0$. This coupling induces a negative null energy in the bulk that shifts the qubit away from the singularity (Fig. 1a), consistent with a quantum computation that recovers the infalling qubit under unitary black hole dynamics[30].

If the sign of the interaction is reversed, the qubit irretrievably falls into the singularity. Wormhole teleportation corresponds to on-shell propagation through the bulk from the left to the right boundary. The

[1]Center for the Fundamental Laws of Nature, Harvard University, Cambridge, MA, USA. [2]Center for Theoretical Physics, Massachusetts Institute of Technology, Cambridge, MA, USA. [3]Division of Physics, Mathematics and Astronomy, Caltech, Pasadena, CA, USA. [4]Alliance for Quantum Technologies (AQT), California Institute of Technology, Pasadena, CA, USA. [5]Google Quantum AI, Venice, CA, USA. [6]Fermilab Quantum Institute and Theoretical Physics Department, Fermi National Accelerator Laboratory, Batavia, IL, USA. [7]These authors contributed equally: Daniel Jafferis, Alexander Zlokapa. ✉e-mail: smaria@caltech.edu

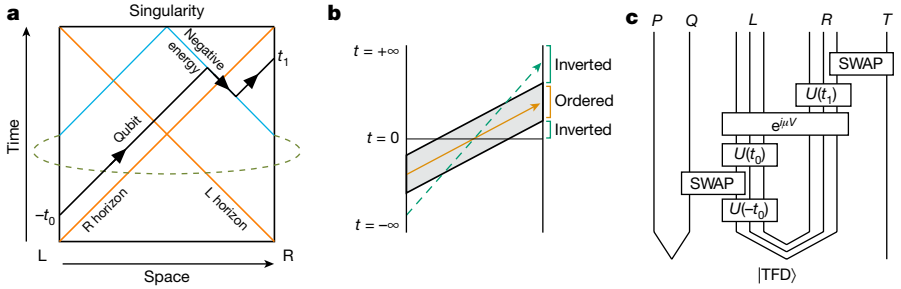

Fig. 1 | Traversable wormhole in spacetime and in the holographic dual. **a**, Diagram of a traversable wormhole in AdS space. A qubit injected at $t = -t_0$ enters through the left side of the wormhole; at $t = 0$, a coupling (dashed line) is applied between the two sides of the wormhole, causing a negative energy shockwave (blue); the qubit experiences a time advance on contact with the shockwave, causing it to emerge from the right side at $t = t_1$. **b**, Illustration of time-ordering (wormhole) and time-inversion (scrambling) of teleportation signals. The smooth semiclassical geometry of a traversable wormhole produces a regime of teleportation that obeys causality; non-gravitational teleportation causes the signals to arrive in reverse order. **c**, The traversable wormhole expressed as a quantum circuit, equivalent to the gravitational picture in the semiclassical limit of an infinite number of qubits. Register P holds a reference qubit entangled with a qubit on register Q that is inserted into the wormhole. The unitary $U(t)$ denotes time evolution $e^{-i(H_L+H_R)t}$ under the left and right SYK models (registers L and R). The TFD state (|TFD〉) initializes the wormhole at $t = 0$. The time evolution and Majorana fermion swap gates achieve qubit injection (register Q) and arrival readout (register T) at the appropriate times. When $\mu < 0$, the coupling $e^{i\mu V}$ generates a negative energy shockwave, allowing traversability; when $\mu > 0$, the coupling generates a positive energy shockwave and the qubit falls into the singularity.

time-ordering of the transmitted quantum information is then preserved through the wormhole (Fig. 1b), unlike teleportation by random unitary dynamics[13,31–34].

Here, we study the dynamics of traversable wormholes through a many-body simulation of an SYK system of N fermions[2,3]. The traversable wormhole protocol is equivalent to a quantum teleportation protocol in the large-N semiclassical limit (Fig. 1c). Explicitly, given left and right Hamiltonians H_L and H_R with N Majorana fermions ψ on each side, the SYK model with q couplings is given by

$$H_{L,R} = \sum_{1 \le j_1 < \cdots < j_q \le N} J_{j_1 \ldots j_q} \psi^{j_1}_{L,R} \cdots \psi^{j_q}_{L,R}, \qquad (1)$$

where the couplings are chosen from a Gaussian distribution with mean zero and variance $J^2(q-1)!/N^{q-1}$. We choose $q = 4$ and demonstrate gravitational physics at sufficiently small N, sparsifying $J_{j_1 \ldots j_q}$ to enable experimental implementation.

To implement the quantum teleportation protocol, we initialize the TFD state $|\mathrm{TFD}\rangle = \frac{1}{\sqrt{Z}} \sum_n e^{-\beta E_n/2} |n\rangle_L \otimes |n\rangle_R$, where $|n\rangle_{L,R}$ are the energy eigenstates of the left and right SYK systems. To swap in a qubit at $t = -t_0$, the system is time-evolved by e^{-iHt} for $H \equiv H_L + H_R$.

At $t = 0$, the interaction $e^{i\mu V}$ is applied across both the left and right subsystems with coupling operator $V = \frac{1}{qN} \sum_j \psi^j_L \psi^j_R$. The sign of μ must be negative to produce a negative energy shockwave that allows the qubit to travel through the wormhole. We note that the fermionic interaction only permits teleportation through a quantum channel, in contrast to a bosonic interaction. We measure the mutual information I_{PT} given by

$$I_{PT}(t) = S_P(t) + S_T(t) - S_{PT}(t), \qquad (2)$$

where S is a measure of entropy. If a quantum system were to teleport by scrambling rather than traversing a wormhole, the mutual information would be symmetric in μ. No information is transmitted when I_{PT} is zero. A peak in I_{PT} is an indication of quantum teleportation in a certain time window.

When $\mu < 0$, mutual information is expected to peak around the scrambling time in the limit of large N. The peaking behaviour of $I_{PT}(t)$ may be observed in two ways: either by setting the injection and readout times to be symmetric ($t \equiv t_0 = t_1$), or by fixing the time of injection (fixed t_0) and measuring different readout times ($t \equiv t_1$). In the semiclassical gravity description, a pole in the causal left-right propagator corresponds to timelike geodesics connecting the left and right

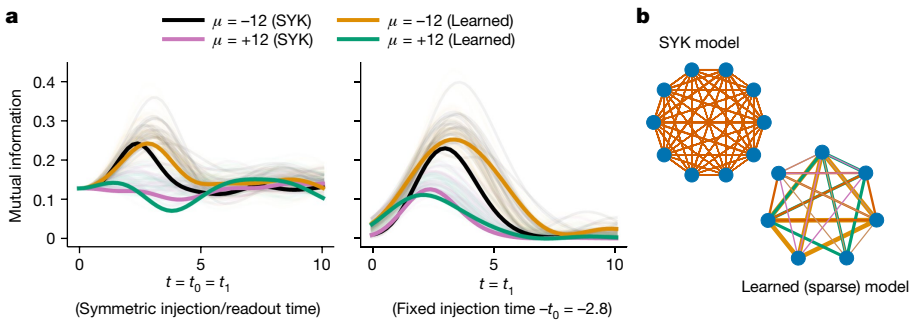

Fig. 2 | Learning a traversable wormhole Hamiltonian from the SYK model. **a**, Mutual information of multiple $N = 10$ SYK models (black and purple, $\beta = 4$) and corresponding learned Hamiltonians (orange and green) showing asymmetry in coupling with $\mu < 0$ (wormhole teleportation) and $\mu > 0$ (scrambling teleportation). Thick lines show a specific instantiation of an SYK model and its corresponding learned sparsification with five non-zero coefficients (equation (3)); light lines indicate a population of SYK models and learned sparsifications with 5–10 non-zero coefficients, demonstrating the reliability of the learning procedure. The learned Hamiltonian is trained only on the mutual information $I_{PT}(t)$ for $t \equiv t_0 = t_1$ (left), and its behaviour is consistent with the wormhole after a qubit is injected at fixed $-t_0$ (right). **b**, Sparsification of the original SYK model with 210 non-zero coefficients (top) to the learned Hamiltonian with five non-zero coefficients (bottom, equation (3)). Groups of four Majorana fermions (blue dots) are coupled with coefficients. Line thickness indicates coefficient magnitude, and colour distinguishes individual coefficients (bottom only).

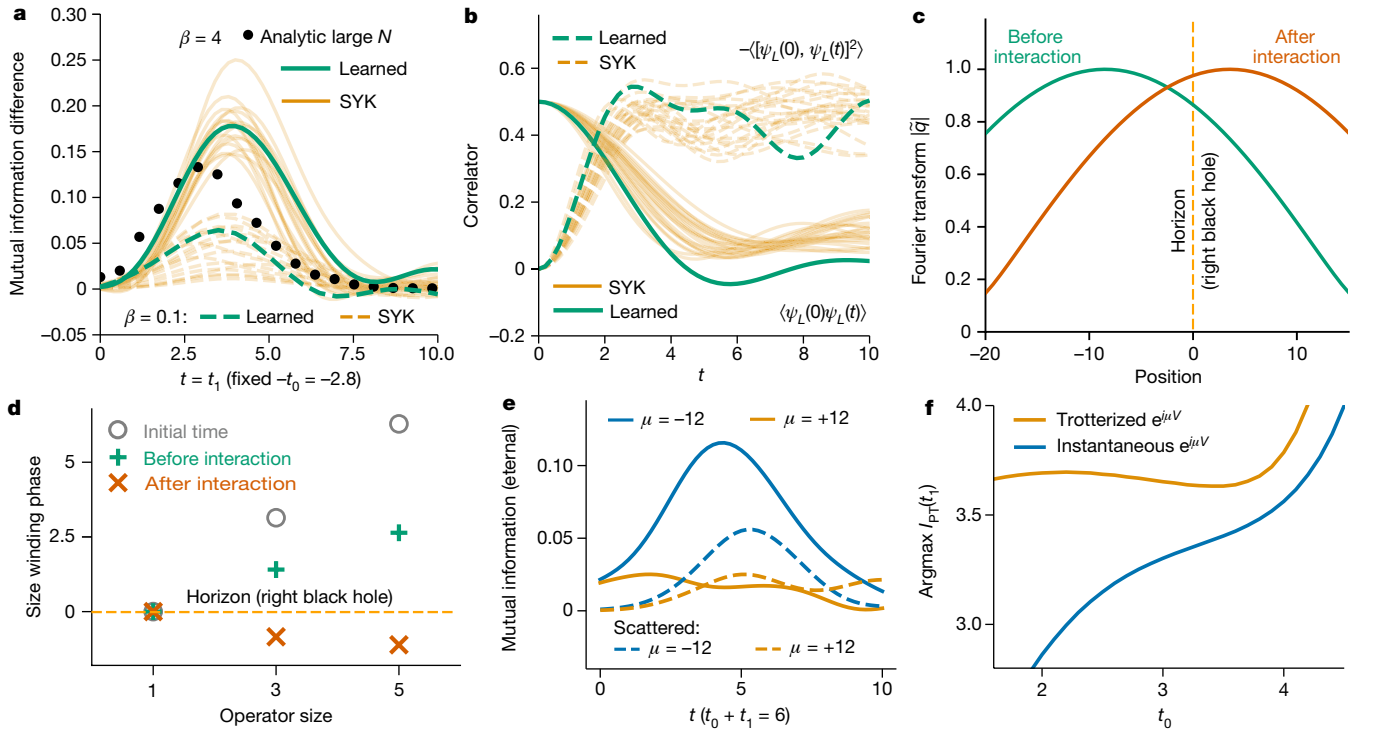

Fig. 3 | Signatures of wormhole traversability for the learned Hamiltonian. **a**, Mutual information asymmetry $I_{\mu<0}(t) - I_{\mu>0}(t)$ for the learned (green) and SYK Hamiltonians (orange) at the low-temperature gravitational limit (solid, $\beta = 4$) and high-temperature scrambling limit (dashed, $\beta = 0.1$). An analytic computation in the large-N limit of the SYK model using chord diagrams (black) is shown for low temperatures, showing agreement with the peak position and height. **b**, Two-point function (solid) and four-point function (dashed), indicating thermalization time and scrambling time respectively of the SYK (orange) and learned (green) Hamiltonians. **c**, Bulk location of the infalling particle before and after the interaction with respect to the black hole horizon, as given by the Fourier transform $|\tilde{q}|$ of the winding size distribution. **d**, Perfect size winding at $t = 0$ (grey), and at $t = 2.8$ before (green) and after (brown) the interaction ($\mu = -12$). As time proceeds, the infalling particle approaches the horizon, as seen by the decreasing slope. Applying the interaction causes the direction of size winding to reverse, corresponding to the particle crossing the horizon in the bulk. **e**, Shapiro time delay in the eternal traversable wormhole protocol caused by scattering in the bulk. The peak shifts right when another qubit is sent through the wormhole in the opposite direction (dashed) compared to sending a single qubit from left to right (solid). The peak height is also reduced due to inelastic scattering. **f**, Causally time-ordered teleportation. The position of the mutual information peak is shown for an instantaneous at $t = 0$ (blue) and prolonged (orange) interaction over $t \in [-1.6, 1.6]$. A positive slope indicates time-inverted teleportation and a negative slope indicates time-ordered teleportation. When the coupling is applied over a window of time, the time-ordering of signals confirms through-the-wormhole behaviour. When the coupling is instantaneous, the decreased slope suggests a combination of teleportation by scrambling and by traversing the wormhole.

systems—that is, a traversable wormhole in the bulk geometry[10]. Hence, we expect the teleportation signal to be maximized when $t_0 \cong t_1 \cong t_*$ for scrambling time t_*. We measure the corresponding peak signature in $I_{PT}(t)$ for both $t \equiv t_0 = t_1$ and $t \equiv t_1$ (fixed t_0). Our numerical simulation shows that $N = 10$ is sufficient to produce such traversable wormhole behaviour (Fig. 2). This result is reinforced by a theoretical analysis of chord diagrams in the double-scaled limit[35] and comparison to previous numerical results[16,36,37] (Supplementary Information). The circuit depth to experimentally implement an $N = 10$ SYK system remains prohibitive. We turn to sparsification of the SYK system and produce evidence of gravitational physics in the sparsified system.

Sparsification of the SYK system (that is, setting many $J_{j_1 \ldots j_4}$ to zero) is shown to preserve gravitational physics even when the number of terms in the Hamiltonian is randomly reduced from $O(N^4)$ to kN with k of order unity[38–40]. Here, we apply techniques from machine learning to optimize the sparsification procedure. The result reduces an $N = 10$ SYK model with 210 terms to an $N = 7$ model with five terms, yielding a nine-qubit circuit for the wormhole teleportation protocol. Whereas larger Hamiltonians may provide a stronger teleportation signal, more gates at current hardware fidelity further attenuate the signal (Supplementary Information); hence, we restrict our attention to the smallest sparsified model with gravitational properties and do not enter the beyond-classical regime.

We construct an analogue of training a neural network. Owing to unitarity and differentiability of the quantum circuit, backpropagation across the wormhole teleportation protocol allows gradient descent to optimize the $J_{j_1 \ldots j_4}$ coefficients with regularization, interpreting the Hamiltonian coefficients as neural network weights. The dataset consists of $I_{PT}(t)$ with $t \equiv t_0 = t_1$ for a standard wormhole constructed by the SYK model with Gaussian-distributed coefficients. The loss function is chosen to be the total mean squared error of $I_{PT}(t)$ for both positive and negative values of a fixed interaction coupling μ, where μ is chosen to maximize the mutual information. Training with weight regularization and truncation sparsifies the Hamiltonian while preserving mutual information dynamics.

Applying the learning process, we produce a large population of sparse Hamiltonians showing the appropriate interaction sign dependence (Fig. 2a). We select the learned Hamiltonian

$$H_{L,R} = -0.36\psi^1\psi^2\psi^4\psi^5 + 0.19\psi^1\psi^3\psi^4\psi^7 - 0.71\psi^1\psi^3\psi^5\psi^6 + 0.22\psi^2\psi^3\psi^4\psi^6 + 0.49\psi^2\psi^3\psi^5\psi^7, \quad (3)$$

which requires seven of the original $N = 10$ SYK model fermions, where ψ^j denotes the Majorana fermions of either the left or the right systems.

To determine whether the sparse learned Hamiltonian describes gravitational physics, we examine equation (3) through two orthogonal approaches: first, we verify that it replicates relevant dynamics of the dense SYK Hamiltonian; and second, we evaluate whether it satisfies necessary criteria of general holographic systems. These criteria

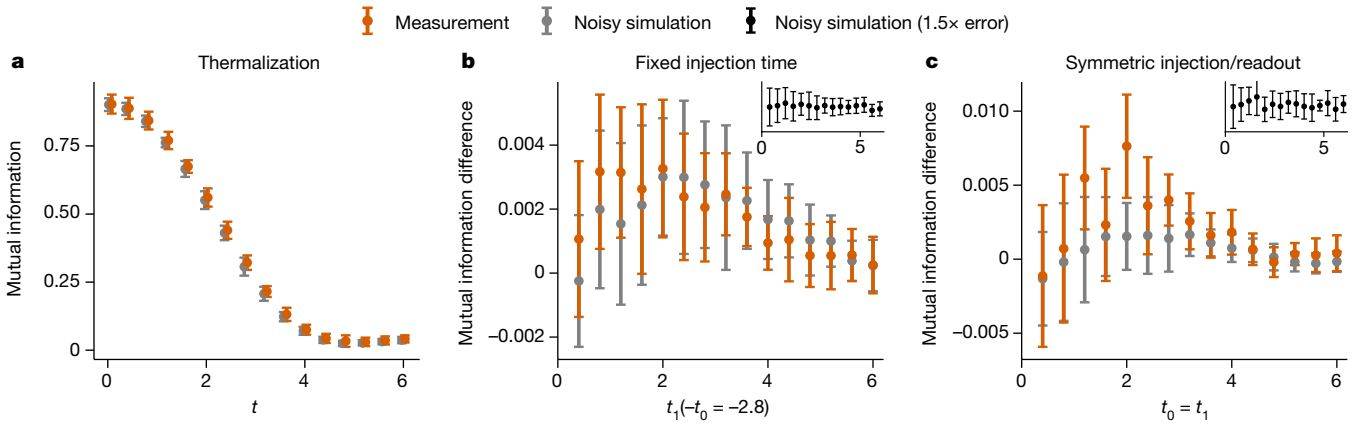

Fig. 4 | Observation of traversable wormhole dynamics. a, Thermalization protocol (109 controlled-Z gates), measuring the mutual information between a qubit injected into a sparse SYK model at time $-t$ and at t. Error bars show three standard deviations over 20 runs. **b**, Traversable wormhole with fixed injection time (164 controlled-Z gates), showing the difference in mutual information between $\mu = -12$ and $\mu = +12$. Error bars show one standard deviation over 28 runs. **c**, Traversable wormhole with symmetric injection and readout time (164 controlled-Z gates), showing the difference in mutual information between $\mu = -12$ and $\mu = +12$. Error bars show one standard deviation over 20 runs. Insets show noisy simulations with gate errors increased by a factor of 1.5, plotted with y axis mutual information range $[-3 \times 10^{-3}, 3 \times 10^{-3}]$; the peak is not visible. The measurements in **b** and **c** agree with noisy simulation and reproduce the sign asymmetry of the mutual information consistent with through-the-wormhole teleportation. The scrambling–unscrambling dynamics of wormhole teleportation cause the mutual information to be substantially attenuated by noise. In noisy simulations, each gate is subjected to depolarization error determined by calibration data (median controlled-Z error 0.3%). Each run consists of 90,000 measurements.

are stricter than the similarity of dynamical observables: they include perfect size winding—the strongest form of size winding that provides a geometric interpretation[11–13]—the causal time-ordering of teleported signals, which shows that the teleportation is not occurring because of random scrambling, and a time delay predicted by scattering in the bulk.

The learned Hamiltonian is consistent with gravitational dynamics of the dense SYK Hamiltonian beyond its training data. The mutual information $I_{PT}(t_1)$ for fixed t_0 shows behaviour compatible with a qubit emerging from a traversable wormhole (Fig. 2a). The mutual information peak height and position strongly resemble the large-N SYK model computation in the double-scaled limit (Fig. 3a). In the high-temperature limit, the mutual information asymmetry between couplings with $\mu < 0$ and $\mu > 0$ diminishes, corresponding to teleportation occurring by means of scrambling instead of through the wormhole, consistent with theoretical expectations[9]. Furthermore, the learned Hamiltonian scrambles and thermalizes similarly to the original SYK model as characterized by the four- and two-point correlators $-\langle[\psi(0), \psi(t)]^2\rangle$ and $\langle\psi(0)\psi(t)\rangle$ (Fig. 3b). Because the scrambling time is roughly equal to the thermalization time, the gravitational interpretation suggests the boundary lies near the horizon.

Beyond comparison to the dense SYK model, we proceed to evaluate more general behaviour predicted from gravity. The property of 'perfect' size winding provides a necessary condition for traversable wormhole behaviour, holding for quantum systems with a nearly AdS_2 bulk[11–13]. Perfect size winding is equivalent to a maximal Lyapunov exponent at large N, but unlike the Lyapunov exponent, size winding remains a meaningful quantity at small N. Non-gravitational systems, such as random non-local Hamiltonians, may teleport in the low-temperature limit with a weak asymmetry in μ; unlike gravitational systems, these have 'imperfect' size winding. Systems that teleport in the high-temperature fully scrambled regime, such as random circuits[34] or chaotic spin chains, do not show any size winding.

Given the thermal state $\rho_\beta \propto e^{-\beta H_L}$, size winding describes the decomposition $\rho_\beta^{1/2}\psi_L^1(t) = \sum_P c_P(t)\psi_L^P$ over strings of $|P|$ fermions. The system shows perfect size winding at time t if the c_P^2 coefficients have a phase that linearly depends on $|P|$. For the Hamiltonian in equation (3), an injected fermion is supported by operators of three sizes.

We find that the learned Hamiltonian has size winding, that is, phases linear in size. As time proceeds, the size winding slope decreases, then flips upon application of the interaction (Fig. 3c,d). The geometric interpretation of the learned Hamiltonian is provided by the Fourier transform, where the bulk location of the infalling particle is seen to approach, then cross the horizon. This analysis shows that teleportation under the learned Hamiltonian is caused by the size winding mechanism, not by generic chaotic dynamics, direct swapping or other non-gravitational dynamics (Supplementary Information).

The Hamiltonian is shown to adhere to the microscopic mechanism of wormhole teleportation through its perfect size winding description. To observe this at a macroscopic scale, we examine two phenomena: a Shapiro time delay and causal time-ordering of signals. For the time delay, we interrogate the learned Hamiltonian within the eternal traversable wormhole framework[15] (Supplementary Information). Besides sending a single qubit from left to right, we insert another qubit across the wormhole from right to left. From a gravitational perspective, this should cause the left-to-right signal to arrive later due to scattering in the bulk. We observe this in the learned Hamiltonian (Fig. 3e). For causal time-ordering, we inspect the order in which infalling particles emerge from the wormhole. If a geometric interpretation is valid, infalling particles should arrive in a causally consistent order (Fig. 1b): signals must emerge in the same order they enter (time-ordered teleportation). By contrast, teleportation in the fully scrambled regime produces a time-inverted ordering of signals. Our learned Hamiltonian generates time-ordered teleportation (Fig. 3f).

The above analyses demonstrate gravitational teleportation by the learned Hamiltonian by means of an emergent wormhole; further analyses examining spectral characteristics, dynamics at different temperatures and interaction strengths, and further properties of size winding are provided in the Supplementary Information. Here, we proceed with a quantum experiment. Namely, we realize the entangled system on the Google Sycamore superconducting qubit array[27] with a nine-qubit circuit of 164 controlled-Z gates and 295 single-qubit gates. We initialize the protocol of Fig. 1c by preparing the TFD state using a hardware-efficient variational quantum eigensolver[41] as the ground state of coupled SYK models[15,42]. Time evolution and the interaction e^{iuV} are applied with a single Trotter step. This is sufficient to achieve a close approximation for the relevant range of t, that is, the number of gates remains constant for all times.

A noisy simulation assuming all gate errors are depolarizing noise agrees with the experimental measurement of the quantum system

as shown in Fig. 4. A simpler protocol measuring thermalization with 109 controlled-Z gates (Fig. 4a) demonstrates the high fidelity of the experiment; more experiments with $\mu = 0$ confirm that coherent errors are dominated by the true teleportation signal (Supplementary Information).

Measuring the traversable wormhole protocol (Fig. 4b,c), we observe increased teleportation when the interaction introduces a negative energy shockwave rather than a positive one. The asymmetric signature is consistent with the physical interpretation that the qubit underwent teleportation through the wormhole. The scrambling–unscrambling dynamics of wormhole teleportation is sensitive to errors: at gate error rates larger than our experiment by a factor of 1.5, the asymmetric wormhole peak-like signal cannot be resolved (Fig. 4 insets). We report median controlled-Z gate errors of 0.3% from simultaneous cross-entropy benchmarking.

We find that the protocol is efficiently scalable to larger system sizes. To satisfy limitations of current quantum hardware, we adopted techniques from machine learning to construct a small-N sparse Hamiltonian that preserves gravitational physics. For systems with $N = O(50)$ fermions, random sparsification is as effective as optimal sparsification up to an order unity constant[38–40] (Supplementary Information). This removes the need for classical simulation without introducing significant overhead, successfully extending to the beyond-classical regime.

This work is a successful attempt at observing traversable wormhole dynamics in an experimental setting. Looking forwards, we anticipate that near-term quantum computers that extend beyond the capabilities of classical simulation will coincide with system sizes that provide new gravitational insight. At too large a value of N, semiclassical gravity describes system dynamics; at too small a value of N, relevant features may not be resolvable.

In the regime of $N = O(100)$ fermions, measurement of inelastic effects in the bulk may provide quantitative insights into aspects of quantum gravity that are poorly understood from a theoretical perspective, such as string production and finite-N corrections to scattering. In our current low N limit implementation, the signal strength from our experiment is rather low. Future experimental work should test the signal amplification as N increases. The use of state-of-the-art noisy intermediate-scale quantum error-mitigation techniques such as the ones developed in refs. [43–46] will be essential in scaling up the experiment. Further to this, implementation of our experiment in other platforms is critical for validation and verification of our observations. The demonstrated approach in this work, of on-chip quantum experimentation of gravity, promises future insights into the holographic correspondence.

Online content

Any methods, additional references, Nature Portfolio reporting summaries, source data, extended data, supplementary information, acknowledgements, peer review information; details of author contributions and competing interests; and statements of data and code availability are available at https://doi.org/10.1038/s41586-022-05424-3.

1. Maldacena, J. The large-N limit of superconformal field theories and supergravity. *Int. J. Theor. Phys.* **38**, 1113–1133 (1999).
2. Sachdev, S. & Ye, J. Gapless spin-fluid ground state in a random quantum Heisenberg magnet. *Phys. Rev. Lett.* **70**, 3339–3342 (1993).
3. Kitaev, A. A simple model of quantum holography. In *Proc. KITP: Entanglement in Strongly-Correlated Quantum Matter* 12 (eds Grover, T. et al.) 26 (Univ. California, Santa Barbara, 2015).
4. Maldacena, J. & Stanford, D. Remarks on the Sachdev-Ye-Kitaev model. *Phys. Rev. D* **94**, 106002 (2016).
5. Almheiri, A. & Polchinski, J. Models of AdS_2 backreaction and holography. *J. High Energy Phys.* **11**, 014 (2015).
6. Gross, D. J. & Rosenhaus, V. The bulk dual of SYK: cubic couplings. *J. High Energy Phys.* **05**, 092 (2017).
7. Maldacena, J. & Susskind, L. Cool horizons for entangled black holes. *Fortschr. Phys.* **61**, 781–811 (2013).
8. Susskind, L. Dear qubitzers, GR=QM. Preprint at https://doi.org/10.48550/arXiv.1708.03040 (2017).
9. Gao, P. & Jafferis, D. L. A traversable wormhole teleportation protocol in the SYK model. *J. High Energy Phys.* **2021**, 97 (2021).
10. Maldacena, J., Stanford, D. & Yang, Z. Diving into traversable wormholes. *Fortschr. Phys.* **65**, 1700034 (2017).
11. Brown, A. R. et al. Quantum gravity in the lab: teleportation by size and traversable wormholes. Preprint at https://doi.org/10.48550/arXiv.1911.06314 (2021).
12. Nezami, S. et al. Quantum gravity in the lab: teleportation by size and traversable wormholes, part II. Preprint at https://doi.org/10.48550/arXiv.2102.01064 (2021).
13. Schuster, T. et al. Many-body quantum teleportation via operator spreading in the traversable wormhole protocol. *Phys. Rev. X* **12**, 031013 (2022).
14. Gao, P., Jafferis, D. L. & Wall, A. C. Traversable wormholes via a double trace deformation. *J. High Energy Phys.* **2017**, 151 (2017).
15. Maldacena, J. & Qi, X.-L. Eternal traversable wormhole. Preprint at https://doi.org/10.48550/arXiv.1804.00491 (2018).
16. Cotler, J. S. et al. Black holes and random matrices. *J. High Energy Phys.* **2017**, 118 (2017).
17. Kitaev, A. & Suh, S. J. The soft mode in the Sachdev-Ye-Kitaev model and its gravity dual. *J. High Energy Phys.* **2018**, 183 (2018).
18. Berkooz, M., Narayan, P., Rozali, M. & Simón, J. Higher dimensional generalizations of the SYK model. *J. High Energy Phys.* **01**, 138 (2017).
19. Witten, E. An SYK-like model without disorder. *J. Phys. A.* **52**, 474002 (2019).
20. Witten, E. Anti-de Sitter space and holography. *Adv. Theor. Math. Phys.* **2**, 253–291 (1998).
21. Gubser, S., Klebanov, I. & Polyakov, A. Gauge theory correlators from non-critical string theory. *Phys. Lett. B.* **428**, 105–114 (1998).
22. Hochberg, D. & Visser, M. The null energy condition in dynamic wormholes. *Phys. Rev. Lett.* **81**, 746–749 (1998).
23. Morris, M. S., Thorne, K. S. & Yurtsever, U. Wormholes, time machines, and the weak energy condition. *Phys. Rev. Lett.* **61**, 1446–1449 (1988).
24. Visser, M., Kar, S. & Dadhich, N. Traversable wormholes with arbitrarily small energy condition violations. *Phys. Rev. Lett.* **90**, 201102 (2003).
25. Visser, M. *Lorentzian Wormholes: From Einstein to Hawking. Computational and Mathematical Physics* (American Institute of Physics, 1995).
26. Graham, N. & Olum, K. D. Achronal averaged null energy condition. *Phys. Rev. D* **76**, 064001 (2007).
27. Arute, F. et al. Quantum supremacy using a programmable superconducting processor. *Nature* **574**, 505–510 (2019).
28. Maldacena, J., Stanford, D. & Yang, Z. Conformal symmetry and its breaking in two dimensional nearly anti-de-Sitter space. *Prog. Theor. Exp. Phys.* **2016**, 12C104 (2016).
29. Maldacena, J. Eternal black holes in anti-de sitter. *J. High Energy Phys.* **2003**, 021–021 (2003).
30. Hayden, P. & Preskill, J. Black holes as mirrors: quantum information in random subsystems. *J. High Energy Phys.* **2007**, 120 (2007).
31. Susskind, L. & Zhao, Y. Teleportation through the wormhole. *Phys. Rev. D* **98**, 046016 (2018).
32. Gao, P. & Liu, H. Regenesis and quantum traversable wormholes. *J. High Energy Phys.* **10**, 048 (2019).
33. Yoshida, B. & Yao, N. Y. Disentangling scrambling and decoherence via quantum teleportation. *Phys. Rev. X* **9**, 011006 (2019).
34. Landsman, K. A. et al. Verified quantum information scrambling. *Nature* **567**, 61–65 (2019).
35. Berkooz, M., Isachenkov, M., Narovlansky, V. & Torrents, G. Towards a full solution of the large N double-scaled SYK model. *J. High Energy Phys.* **03**, 079 (2019).
36. García-García, A. M. & Verbaarschot, J. J. M. Spectral and thermodynamic properties of the Sachdev-Ye-Kitaev model. *Phys. Rev. D* **94**, 126010 (2016).
37. García-García, A. M. & Verbaarschot, J. J. M. Analytical spectral density of the Sachdev-Ye-Kitaev model at finite *n*. *Phys. Rev. D* **96**, 066012 (2017).
38. Xu, S., Susskind, L., Su, Y. & Swingle, B. A sparse model of quantum holography. Preprint at https://doi.org/10.48550/arXiv.2008.02303 (2020).
39. Garcia-Garcia, A. M., Jia, Y., Rosa, D. & Verbaarschot, J. J. M. Sparse Sachdev-Ye-Kitaev model, quantum chaos, and gravity duals. *Phys. Rev. D* **103**, 106002 (2021).
40. Caceres, E., Misobuchi, A. & Pimentel, R. Sparse SYK and traversable wormholes. *J. High Energy Phys.* **11**, 015 (2021).
41. Kandala, A. et al. Hardware-efficient variational quantum eigensolver for small molecules and quantum magnets. *Nature* **549**, 242–246 (2017).
42. Cottrell, W., Freivogel, B., Hofman, D. M. & Lokhande, S. F. How to build the thermofield double state. *J. High Energy Phys.* **2019**, 58 (2019).
43. Huggins, W. J. et al. Virtual distillation for quantum error mitigation. *Phys. Rev. X* **11**, 041036 (2021).
44. O'Brien, T. E. et al. Error mitigation via verified phase estimation. *PRX Quantum* **2**, 020317 (2021).
45. Temme, K., Bravyi, S. & Gambetta, J. M. Error mitigation for short-depth quantum circuits. *Phys. Rev. Lett.* **119**, 180509 (2017).
46. Li, Y. & Benjamin, S. C. Efficient variational quantum simulator incorporating active error minimization. *Phys. Rev. X* **7**, 021050 (2017).

Data availability

Data from this work are available upon request.

Code availability

Code from this work is available upon request.

47. Kolchmeyer, D. K. *Toy Models of Quantum Gravity*. PhD thesis, Harvard Univ. (2022); https://nrs.harvard.edu/URN-3:HUL.INSTREPOS:37372099.
48. Zlokapa, A. *Quantum Computing for Machine Learning and Physics Simulation*. BSc thesis, California Institute of Technology (2021); https://doi.org/10.7907/q75q-zm20.

Acknowledgements The experiment was performed in collaboration with the Google Quantum AI hardware team, under the direction of A. Megrant, J. Kelly and Y. Chen. We acknowledge the work of the team in fabricating and packaging the processor; building and outfitting the cryogenic and control systems; executing baseline calibrations; optimizing processor performance and providing the tools to execute the experiment. Specialized device calibration methods were developed by the physics team led by V. Smelyanskiy. We in particular thank X. Mi and P. Roushan for their technical support in carrying out the experiment and are grateful to B. Kobrin for useful discussions and validation studies. This work is supported by the Department of Energy Office of High Energy Physics QuantISED programme grant no. SC0019219 on Quantum Communication Channels for Fundamental Physics. Furthermore, A.Z. acknowledges support from the Hertz Foundation, the Department of Defense through the National Defense Science and Engineering Graduate Fellowship Program, and Caltech's Intelligent Quantum Networks and Technologies research programme. S.I.D. is partially supported by the Brinson Foundation. Fermilab is operated by Fermi Research Alliance, LLC under contract number DE-AC02-07CH11359 with the United States Department of Energy. We are grateful to A. Kitaev, J. Preskill, L. Susskind, P. Hayden, A. Brown, S. Nezami, J. Maldacena, N. Yao, K. Thorne and D. Gross for insightful discussions and comments that helped us improve the manuscript. We are also grateful to graduate student O. Cerri for the error analysis of the experimental data. M.S. thanks the members of the QCCFP (Quantum Communication Channels for Fundamental Physics) QuantISED Consortium and acknowledges P. Dieterle for the thorough inspection of the manuscript.

Author contributions J.D.L. and D.J. are senior co-principal investigators of the QCCFP Consortium. J.D.L. worked on the conception of the research program, theoretical calculations, computation aspects, simulations and validations. D.J. is one of the inventors of the SYK traversable wormhole protocol. He worked on all theoretical aspects of the research and the validation of the wormhole dynamics. Graduate student D.K.K.[47] worked on theoretical aspects and calculations of the chord diagrams. Graduate student S.I.D. worked on computation and simulation aspects. Graduate student A.Z.[48] worked on all theory and computation aspects, the learning methods that solved the sparsification challenge, the coding of the protocol on the Sycamore and the coordination with the Google Quantum AI team. Postdoctoral scholar N.L. worked on the working group coordination aspects, meetings and workshops, and follow-up on all outstanding challenges. Google's VP Engineering, Quantum AI, H.N. coordinated project resources on behalf of the Google Quantum AI team. M.S. is the lead principal investigator of the QCCFP Consortium Project. She conceived and proposed the on-chip traversable wormhole research program in 2018, assembled the group with the appropriate areas of expertise and worked on all aspects of the research and the manuscript together with all authors.

Competing interests The authors declare no competing interests.

Additional information

Supplementary information The online version contains supplementary material available at https://doi.org/10.1038/s41586-022-05424-3.

Correspondence and requests for materials should be addressed to Maria Spiropulu.

Peer review information *Nature* thanks the anonymous reviewers for their contribution to the peer review of this work.